Miner Petrol (2009) 95:303–313
DOI 10.1007/s00710-008-0029-y

ORIGINAL PAPER

Complex chemical zoning in eclogite facies garnet reaction rims: the role of grain boundary diffusion

J. Prenzel · R. Abart · L. Keller

Received: 9 May 2008 / Accepted: 13 October 2008 / Published online: 31 October 2008

Abstract In metapelites of the Saualpe complex (Eastern Alps) continuous 10 μm to 20 μm wide garnet reaction rims formed along biotite-plagioclase and biotite-perthite interfaces. The pre-existing mineral assemblages are remnants of low pressure high temperature metamorphism of Permian age. The garnet reaction rims grew during the Cretaceous eclogite facies overprint. Reaction rim growth involved transfer of Fe and Mg components from the garnet-biotite interface to the garnet-feldspar interface and transfer of the Ca component in the opposite direction. The garnets show complex, asymmetrical chemical zoning, which reflects the relative contributions of short circuit diffusion along grain boundaries within the polycrystalline garnet reaction rims and volume diffusion through the grain interiors on bulk mass transfer. It is demonstrated by numerical modelling that the spacing of the grain boundaries, i.e. the grain size of the garnet in the reaction rim is a first order control on its internal chemical zoning.

Introduction

Metasomatic reaction bands and corona structures are a frequently observed phenomenon in igneous and metamorphic rocks (Joesten 1977). They are usually formed in a pre-existing polyphase mineral assemblage. The rim forming reactions are triggered by changes in the physical and/or chemical conditions, which destabilize the pre-existing mineral or mineral paragenesis. New minerals or mineral assemblages are formed, which tend to bring the system into a new equilibrium configuration. Reaction rims provide evidence for incomplete mineral reactions and the size, spatial distribution, internal chemical zoning and internal microstructure and texture of reaction rims contain important kinetic information (Joesten 1977, Keller et al. 2006, 2008). The analysis of such microstructures may, hence, help to determine reaction rates and to understand the dynamics of geological systems during metamorphism.

Reaction rim formation requires transfer of chemical components between the reactant phases or assemblages. The arrangement of the reaction products in the form of a reaction rim minimizes the transport distances for the necessary chemical mass transfer. Reaction rims are thus an indication of transport controlled mineral reactions (Fisher 1973, Joesten 1977). In the absence of fluid or melt migration, chemical transport most likely occurs by diffusion. At the pressure and temperature conditions of medium to high grade metamorphism diffusion is particularly slow, if water fugacity is low. Reaction rims and corona structures are thus to be expected primarily in "dry" rock systems.

We investigated garnet reaction rims, which were formed in medium to high grade metamorphic metapelites of the Saualpe complex in the Eastern Alps. The rocks of the Saualpe complex had been largely dehydrated in the course of low pressure medium to high grade metamorphism during Permian times. The garnet reaction rims were formed under eclogite-facies conditions during Eo-Alpine metamorphism in the Cretaceous. The garnet rims crystallized at the interfaces between pre-existing medium to coarse-grained biotite and plagioclase or biotite and perthite, which are supposed to have originated during the Permian metamorphic event. Rim growth involved interdiffusion of Fe and Mg components from the biotite and the Ca component from the feldspar.

Editorial handling: D. Harlov

J. Prenzel (✉) · R. Abart · L. Keller
Institute of Geological Sciences, Free University Berlin,
Malteserstraße 74-100,
12249 Berlin, Germany
e-mail: Jannis.Prenzel@web.de

Rim growth was, hence, temperature and time dependent. If the reaction temperature is known, time information can potentially be extracted from this microstructure (Keller et al. 2006, 2008). In this context, knowledge of diffusion mechanisms and pathways of material transport through the growing rim is crucial. The pathways of mass transfer across a reaction rim may be reflected by its internal chemical zoning. We use high resolution element mapping and chemical analysis to investigate the internal chemical zoning of the garnet reaction rims. The observed peculiar asymmetric zoning pattern suggests that grain boundary diffusion contributed substantially to bulk chemical transport across the reaction rim during its growth, as proposed by Keller et al. (2006).

Geological background and metamorphism

The Saualpe complex pertains to the Austroalpine nappe system, which tectonically forms one of the highest and most prominent units in the Eastern Alps (Schmid et al. 2004). The Austroalpine comprises a series of decollement nappes of Permo-Mesozoic sequences, which in places are stratigraphically linked to their low grade metamorphic Paleozoic basement. Large fractions of the Austroalpine nappe system are comprised, however, of polymetamorphic basement rocks. The Kor-Saualpe complex forms a prominent part of this Austroalpine basement east of the Tauern Window (Fig. 1).

At least two pre-Alpine and one eo-Alpine metamorphic events have been identified from mineral parageneses and geochronology in the Austroalpine basement unit E of the Tauern Window. The study of metapelitic rocks and, in particular, the detailed investigation of different generations and growth zones in garnet porphyroblasts have contributed to the unravelling of this complex metamorphic history (Frank et al. 1983, Abart and Martinelli 1989, Schuster and Thöni 1996, Schuster et al. 2001, Gaidies et al. 2006, 2007, Schuster and Stüwe 2008). With respect to pre-Alpine metamorphic evolution, a medium temperature, medium pressure event and a low pressure high temperature event have been discerned (Habler and Thöni 2001, Gaidies et al.

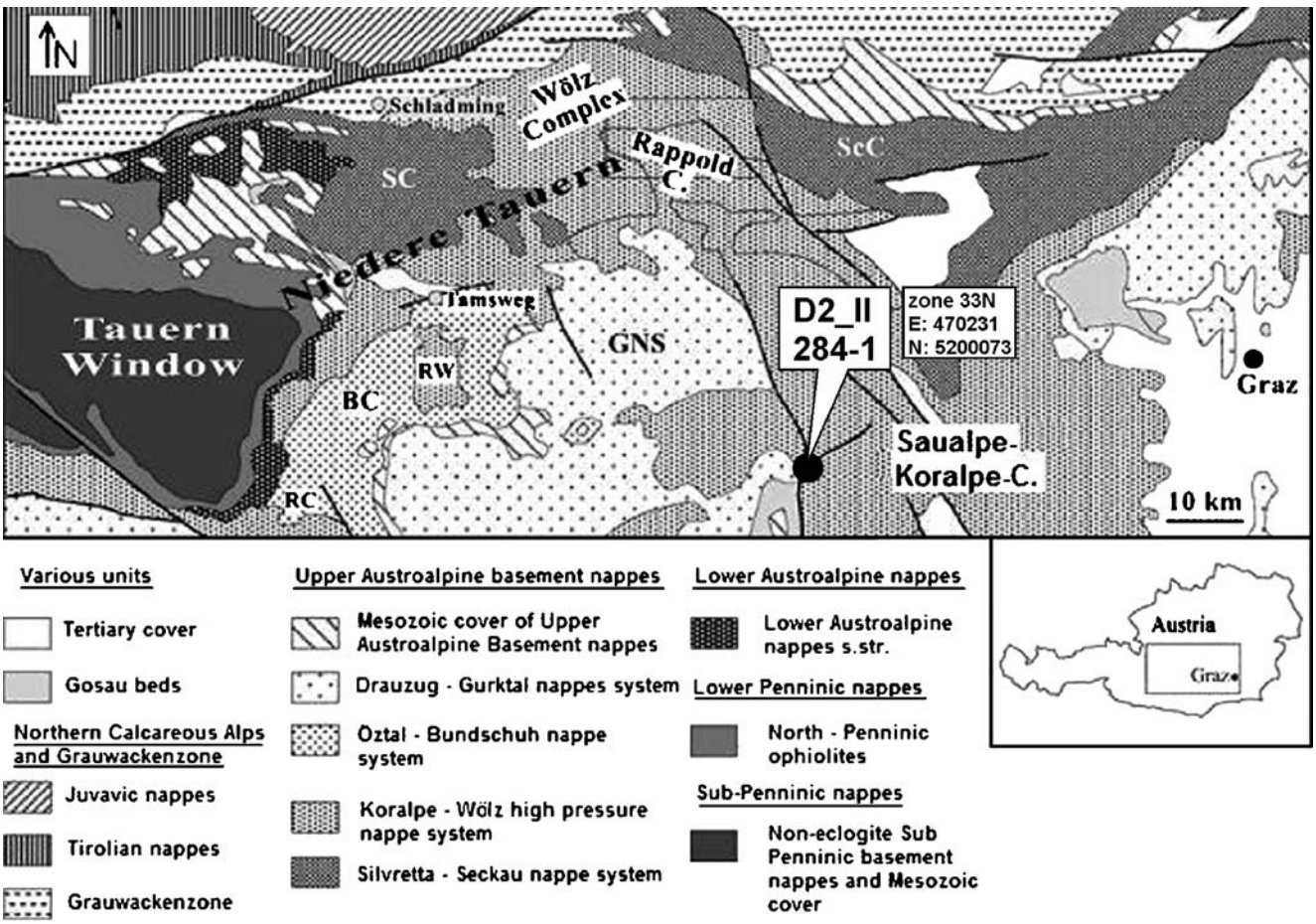

Fig. 1 Simplified geological map of the main tectonic units east of the Tauern Window showing the location of the Koralpe-Saualpe complex and the location of samples D2_II and 284-1 with geographic coordinates (using UTM projection and WGS84 ellipsoid). Modified from Gaidies et al. (2006)

2006, 2007). The medium pressure event reached amphibolite facies conditions and produced a first generation of garnet porphyroblasts as well as staurolite and kyanite. Although unambiguous geochronological data are missing, this event is believed to be of Variscan age based on geological considerations (Frank et al. 1983). The low pressure metamorphic event lead to the formation of garnet in previously unmetamorphosed or low grade metamorphic pelitic rocks. This garnet generation was dated at about 270 Ma (Schuster and Thöni 1996, Lichem et al. 1997, Thöni and Miller 2008). Widespread magmatic activity and pegmatite formation is associated with the low pressure metamorphic event. Emplacement ages of meta igneous rocks, which are related to the Permian low-pressure high-temperature event, range from 275 Ma to 230 Ma (Morauf 1980, 1981, 1982, Paquette and Gebauer 1991, Thöni and Jagoutz 1992, 1993, Heede 1997, Miller and Thöni 1997, Thöni and Miller 2000, Habler and Thöni 2001, Habler et al. 2007).

In the Saualpe region, Pilger and Schönenberg (1975) discern a high grade "Gneiss Unit", a medium grade "Mica schist Unit", and a low grade "Phyllite Unit". The Gneiss Unit, where the investigated rocks have been taken from, consists of paragneisses and shows evidence of eclogite facies metamorphism. In the Gneiss Unit some rocks have been only weakly affected by the eo-Alpine metamorphic overprint and show preservation of relic pre eo-Alpine mineral parageneses and microstructures (Habler and Thöni 2001). This is particularly pronounced in pegmatite gneisses and in Al rich graphitic biotite plagioclase gneisses.

Analytical methods

Mineral chemical analyses, back scattered electron images and element distribution maps were produced on a JEOL-JXA-8200 electron microprobe at the Freie Universität Berlin. Analyses were performed with an acceleration voltage of 15 kV, a beam current of 20 nA and a beam diameter of 1 µm. For element distribution maps the dwell time was set to 100–200 ms per pixel. For quantitative analysis andesine (Ca, Na, Si), clinopyroxene (Al, Mg), chromite (Cr), ilmenite (Ti), magnetite (Fe), orthoclase (K) and rhodonite (Mn) were used as standards.

Element distribution maps with high spatial resolution were produced using a JEOL JXA-8500F thermal field emission electron microprobe at the Deutsches GeoForschungsZentrum in Potsdam. For imaging on the field emission instrument an acceleration voltage of 8 kV, a beam current of 10 nA and a dwell time of 300-400 ms were used.

Petrography

The two studied samples 284-1 and D2_II are metapelites taken from the high grade Gneiss Unit of the Saualpe complex (Fig. 1). Both samples pertain to the corundum bearing biotite-plagioclase gneisses. In these rocks the pre-Alpine mineral paragenesis is relatively well preserved. It is comprised of coarse-grained biotite, plagioclase, perthitic alkali feldspar, white mica, garnet, corundum and kyanite aggregates in the form of µm-sized needles. Apatite, tourmaline, ilmenite, rutile, epidote, graphite and zircon are present as accessory minerals.

In sample 284-1 coarse grained plagioclase is the only feldspar in the pre-Alpine paragenesis. In contrast, both plagioclase and alkali feldspar are present as part of the pre Alpine paragenesis in sample D2_II. The alkali feldspar is orthoclase rich with relatively coarse (several 10's of µm sized) grains of plagioclase with an intermediary composition (Table 1). The plagioclase is partially replaced by white mica. The most conspicuous sign of the eo-Alpine overprint is the formation of garnet reaction rims at former biotite-plagioclase or biotite-perthite interfaces.

The association and the spatial arrangement of biotite, plagioclase/perthite, garnet, white mica/K-feldspar, and quartz suggest garnet forming reactions of the type:

$$plagioclase + biotite = garnet + K - feldspar \qquad \text{type I}$$

or

$$perthite/plagioclase + biotite = garnet + white\,mica + quartz \qquad \text{type II}$$

In the microstructures that are generated by reactions of type I (284-1) the garnet rim is accompanied by a thin (2–5 µm wide), continuous rim of K-feldspar adjacent to the plagioclase (Figs. 2 c,d). In microstructures of reaction type II (D2_II) only garnet is present as a continuous rim. White mica is formed within the plagioclase intergrowths in the perthitic alkali feldspar, and in many cases it completely replaces the plagioclase intergrowths.

Mineral Chemistry

Garnet

Representative analyses of the rim forming garnets are given in Table 1. Garnet (Grt) compositions in the two samples vary between $Py_{0.09}Alm_{0.68}Gro_{0.10}Spe_{0.01}$ and $Py_{0.13}Alm_{0.79}Gro_{0.21}Spe_{0.02}$. Element distribution maps of rim garnets reveal various types of complex chemical zonings (Figs. 2 and 3). Garnet compositions were also analysed quantitatively along profiles across the garnet rims

Table 1 Representative mineral analyses of biotite-plagioclase gneiss

Sample	284-1					D2_II						
	Grt 1 /Pl	Grt 2 /rim	Grt 3 /Bt	Bt	Pl	Grt 1 /Kfs		Grt 2 /rim	Grt 3 /Bt	Ms	Bt	Pl	Kfs
SiO_2	38.01	37.41	37.50	36.47	61.73	SiO_2	37.87	38.52	38.24	47.06	36.69	56.29	64.04
TiO_2	0.00	0.00	0.00	3.57	0.00	TiO_2	0.00	0.00	0.00	0.24	3.05	0.00	0.00
Cr_2O_3	0.00	0.02	0.04	0.00	0.00	Cr_2O_3	0.02	0.00	0.01	0.00	0.00	0.00	0.00
Al_2O_3	21.32	21.65	21.59	19.51	25.00	Al_2O_3	21.63	21.72	21.65	35.94	19.58	28.24	19.37
Fe_2O_3	0.00	0.00	0.00	0.00	0.00	Fe_2O_3	0.10	0.00	0.36	0.00	0.00	0.29	0.00
FeO	33.06	35.47	34.61	20.57	0.14	FeO	30.58	33.13	31.93	1.55	19.70	0.00	0.66
MnO	0.38	0.45	0.43	0.03	0.00	MnO	0.70	0.72	0.77	0.03	0.10	0.00	0.00
MgO	2.43	2.60	2.20	6.08	0.00		MgO	2.61	3.29	2.95	0.51	6.82	0.02
CaO	5.56	3.33	4.41	0.01	6.42	CaO	7.30	4.48	6.06	0.02	0.07	9.42	0.06
Na_2O	0.00	0.00	0.00	0.14	8.03	Na_2O	0.00	0.00	0.00	0.24	0.09	6.03	0.85
K_2O	0.00	0.00	0.00	9.24	0.21	K_2O	0.00	0.00	0.00	10.13	9.09	0.19	14.54
Total	100.75	100.92	100.79	95.64	101.51	Total	100.80	101.85	101.97	95.72	95.18	100.46	99.53
Si	3.02	2.98	2.99	2.76	2.71	Si	2.99	3.02	2.99	3.10	2.78	2.52	2.97
Ti	0.00	0.00	0.00	0.20	0.00	Ti	0.00	0.00	0.00	0.01	0.17	0.00	0.00
Cr	0.00	0.00	0.00	0.00	0.00	Cr	0.00	0.00	0.00	0.00	0.00	0.00	0.00
Al	2.00	2.03	2.03	1.74	1.29	Al	2.01	2.01	2.00	2.79	1.75	1.49	1.06
Fe^{3+}	0.00	0.01	0.00	0.00	0.00	Fe^{3+}	0.01	0.00	0.02	0.00	0.00	0.01	0.00
Fe^{2+}	2.20	2.36	2.31	1.30	0.01	Fe^{2+}	2.02	2.17	2.09	0.09	1.25	0.00	0.03
Mn	0.03	0.03	0.03	0.00	0.00	Mn	0.05	0.05	0.05	0.00	0.01	0.00	0.00
Mg	0.29	0.31	0.26	0.69	0.00	Mg	0.31	0.38	0.34	0.05	0.77	0.00	0.00
Ca	0.47	0.28	0.38	0.00	0.30	Ca	0.62	0.38	0.51	0.00	0.01	0.45	0.00
Na	0.00	0.00	0.00	0.02	0.68	Na	0.00	0.00	0.00	0.03	0.01	0.52	0.08
K	0.00	0.00	0.00	0.89	0.01	K	0.00	0.00	0.00	0.85	0.88	0.01	0.86
Total	8.00	8.00	8.00	7.62	5.00	Total	8.00	8.00	8.00	6.93	7.62	5.00	5.00
Alm	0.74	0.79	0.78	An	0.30	Alm	0.68	0.73	0.70		An	0.46	0.00
Sps	0.01	0.01	0.01	Ab	0.69	Sps	0.02	0.02	0.02		Ab	0.53	0.09
Pyr	0.10	0.10	0.09	Or	0.01	Pyr	0.10	0.13	0.12		Or	0.01	0.91
Grs	0.16	0.10	0.13			Grs	0.21	0.13	0.17				

Mineral formulae were calculated as follows: Grt, Bt, Ms (12 oxygen); Pl, Kfs (eight oxygen).

of samples 284-1 and D2_II (Figs. 2a and 3d). The compositional variations across the rims yielded quite similar chemical profiles for both samples (Figs. 4a,b). There is no difference in the garnet zoning patterns between those at the plagioclase/biotite-interface (Fig. 2b) and those at perthite/biotite-interface (Fig. 3e). All these garnets show a pronouncedly asymmetrical chemical zoning pattern. Generally the garnets are relatively Ca rich towards the interface with the feldspar and relatively Ca poor towards the biotite (Figs. 3b,e,h and 5a,c,d). The transition between the two compositional domains is located approximately along the central axes of the garnet rims. The zoning trends of Fe and Mg are complementary to the Ca concentration (Figs. 3c,f,l and 4a,b). Considering the fact that biotite acted as a source for the FeO and MgO components and plagioclase acted as a source for the CaO component, such a zoning pattern is intuitively expected. Given that the chemical components were most likely redistributed across the rim by volume diffusion, a monotonous decrease of the Ca concentrations from the garnet-feldspar interface towards the garnet-biotite interface would be expected. In some cases, such a zoning pattern is indeed observed (Figs. 3h and 6a,c,d). In many locations, however, the zoning is more complex. In some cases, the highest Ca concentrations are observed in the inner parts of the garnet rim and the Ca concentrations decrease from the inner parts of the rim towards the garnet-perthite interface (Figs. 3h and 5a,b). In addition, the Ca concentrations may be elevated at the garnet-biotite interface over a 5 µm to 10 µm wide zone (Figs. 2b, 3e, 4a,b), which is counter intuitive assuming mass transfer by volume diffusion.

The internal structure of the garnet reaction rims can be described as a composite of garnet grains, which are separated from each other by grain boundaries. In general the intraphase grain boundaries are orientated perpendicular to the garnet rims. The grain boundaries provide short connections between the garnet-biotite and the garnet-feldspar interfaces and are thus potential pathways for short circuit diffusion. A high resolution Ca distribution map of a garnet reaction rim is shown in Fig. 6. There the Ca

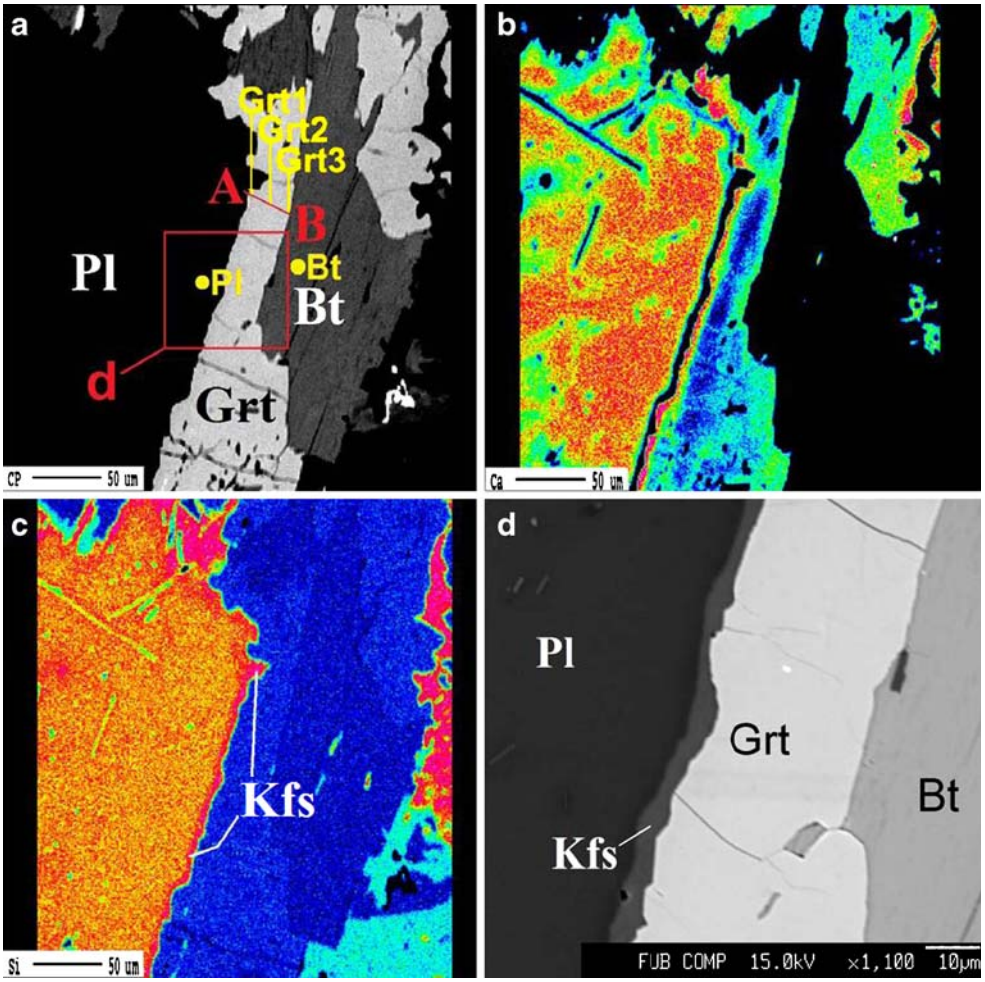

Fig. 2 Chemical zoning of garnet reaction rims from sample 284-1. **a**) Back-scattered electron (BSE) image of the garnet (Grt) reaction rim, which formed along the former biotite-plagioclase (Bt, Pl) interphase boundary. Overview of a quantitative profile (A to B) across a garnet rim and representative analysis points for Pl, Bt and Grt (yellow letters) are shown. Detailed BSE-image of the area marked in red is shown in d. **b**) corresponding element distribution map for Ca. **c**) corresponding element distribution map for Si. **d**) Detailed BSE-image of the area marked in red on a

concentration is slightly elevated with respect to the interior of the rim. Although somewhat overprinted by alteration along a late crack, it is seen that the Ca concentration is elevated also along an elongate zone, which is sub-parallel to the crack. This elongate zone of elevated Ca concentrations is interpreted as a grain boundary within the garnet rim, which served as a pathway for fast diffusion across the rim. Keller et al (2006) could unambiguously identify grain boundaries in a similar setting using EBSD. The slightly elevated Ca concentration within the garnet rim in Fig. 3e could be interpreted as a grain boundary in the same way.

Feldspar

Representative feldspar analyses are given in Table 1. In sample 284-1 feldspar is present as a chemically homogeneous plagioclase (Pl) which is relatively anorthite rich with X_{An}=0.30; X_{Ab}=0.69 and X_{Or}=0.01 (Figs. 2a,b). Only in a several µm wide zone along the interfaces with garnet rims (Grt) or with the K-feldspar (Kfs) rims that locally accompany the garnet rims (Figs. 2c,d) the anorthite component may be reduced substantially (Fig. 2b).

Sample D2_II contains coarse perthites. The plagioclase (Pl) intergrowths have a composition of X_{An}=0.46; X_{Ab}=0.53 and X_{Or}=0.01 and the K-feldspar host (Kfs) has a composition of X_{An}=0.00; X_{Ab}=0.09 and X_{Or}=0.91. The plagioclase intergrowths are partially replaced by white mica (Figs. 3j,k,l).

Conditions of reaction rim formation

The pressure-temperature conditions during the Permian metamorphism of the Saualpe crystalline basement were estimated at 0.4 GPa and 600°C (Habler and Thöni 2001). The conditions of the Eo-Alpine eclogite facies metamorphic overprint in the Kor-Saualpe area have been estimated at about 600+/−20°C and 1.3+/−0.15 GPa (Habler 1999).

Phase diagram calculations were done using the Vertex program of Connolly (1990) and the thermodynamic data from Holland and Powell (1998). Figure 7a, calculated assuming H_2O saturation, shows the phase relations that were calculated for a theoretical bulk rock composition consisting of equal amounts of 1/2 plagioclase and 1/2 biotite and mineral compositions, taken from sample 284-1

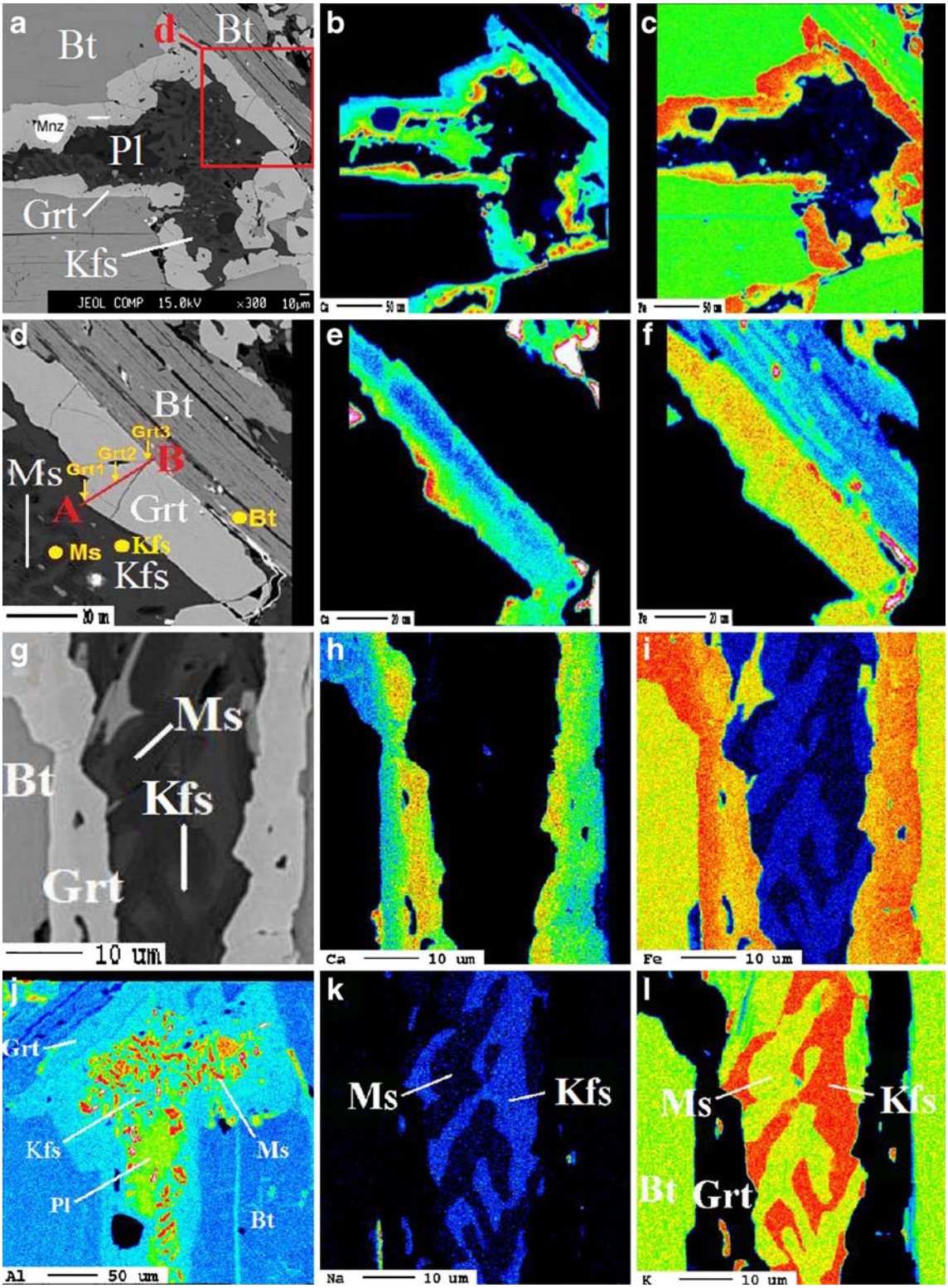

Fig. 3 Chemical zoning of garnet reaction rims from sample D2_II. **a**,**d**, **g**) Back-scattered electron (BSE) images of garnet (Grt) reaction rims, which form along the former biotite-perthite (Bt, Kfs) interphase boundaries. **b**,**e**,**h**) corresponding element distribution maps for Ca. **c**,**f**, **i**) corresponding element distribution maps for Fe. **j**) element distribution map for Al. **k**) element distribution map for Na. **l**) element distribution map for K. Warm colours indicate high concentrations and cold colours indicate low concentrations of the respective elements. Overview of a quantitative profile (A to B) across a garnet rim and points of representative analysis of Kfs, Ms, Bt and Grt (yellow letters) are shown in d

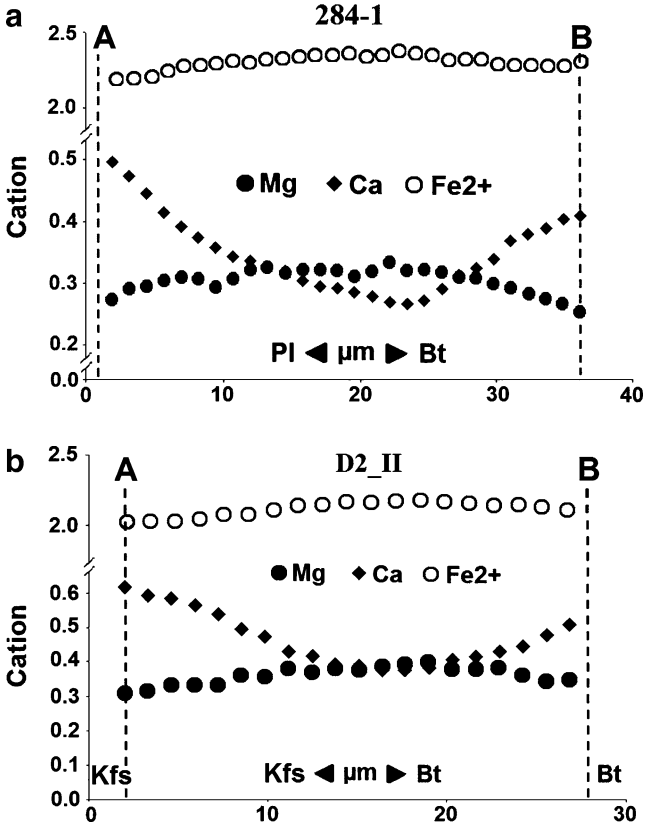

Fig. 4 **a**) Garnet composition along profile A-B from Fig. 2a (**b**) Garnet composition along profile A-B from Fig. 3d. The vertical dashed lines indicate the plagioclase/garnet or perthite/garnet and the garnet/biotite interphase boundaries. The analyses were normalized to a total of 12 oxygens

(Table 1). It is assumed that this bulk composition reflects the thermodynamically stable system required for garnet rim growth. Under conditions of Permian low-pressure, high temperature metamorphism, garnet was not stable. For the given effective bulk composition, garnet was only stabilized at the elevated pressures obtained during the Cretaceous event.

Calculations at reduced water activity indicate that K-feldspar becomes stable in the high pressure assemblage when $aH_2O<0.2$. The diagram in Fig. 7b shows phase relations at $aH_2O=0.1$. Under the conditions of Cretaceous high-pressure metamorphism, sanidine was stable instead of paragonite as in the diagram calculated for water saturation in Fig. 7a. Because K-feldspar is observed as a reaction product during garnet rim growth (see Fig. 2) it is inferred that garnet rims formed at low aH_2O. A system with $aH_2O>0.2$ would not produce K-feldspar. In addition, the sample does not contain paragonite, which would be expected in a water-saturated system at the conditions present during Cretaceous metamorphism (Fig. 7a).

Pseudosection calculations also indicate that plagioclase was higher in An-content at point A at the P-T conditions obtained during Permian low pressure metamorphism than at point B at the P-T conditions present during the eo-Alpine eclogite facies metamorphic overprint. This indicates that plagioclase had the potential to release An-component and may have acted as source for Ca during the eo-Alpine overprint.

Modelling of growth zoning

In order to discern the factors, which controlled the formation of locally different asymmetric growth zonings in the garnet reaction rims for the same sample, we used the numerical model of Keller et al. (2008), which outlines the governing equations and numerical scheme. In this model, the growing reaction rim contains multiple parallel grain boundaries, which are connected to interphase boundaries (Fig. 8a). For the chosen boundary topology, a state can arise where material diffuses out of one of the interphase boundaries between garnet and plagioclase/perthite or garnet and biotite and then diffuses rapidly across the growing reaction rim along the grain boundaries within the garnet polycrystal. As soon as it reaches the interphase boundary on the opposite side, it is efficiently distributed laterally. Because the boundaries are very thin when compared to the size of the model system, these boundaries are treated as surfaces with effective transport properties. The growth rates are controlled by the net flux change across the interphase boundaries as well as by grain and interphase boundary diffusion, which changes the concentrations along the phase boundaries. In addition, adjustment of local equilibrium across the moving boundaries is assumed to occur rapidly.

A consequence of such an interrelation between rim growth and short circuit diffusion is the formation of a characteristic growth zoning in the reaction rim. The zoning characteristics largely depend on the relative contribution of grain boundary diffusion and volume diffusion to the bulk diffusion across the reaction rim but also on the material flux in the reactants towards the reaction interfaces (Keller et al. 2006, 2008). In the applied modelling approach the chemical transport capacities along the grain boundaries depend on the grain boundary diffusion coefficient D^{gb}, the solubility of the diffusing species in the boundary medium, and the boundary width. In the Saualpe rocks we observe different types of zoning within the reaction rims. Because local variations in material properties (i.e. volume and grain boundary diffusivities, grain boundary width and solubility) are unlikely, such differences in the zoning pattern are likely related to local variations in the geometrical factors (e.g. the spacing between the grain boundaries). In order to investigate the influence of geometrical factors on the zoning characteristics, the parameters related to material properties were set to fixed values.

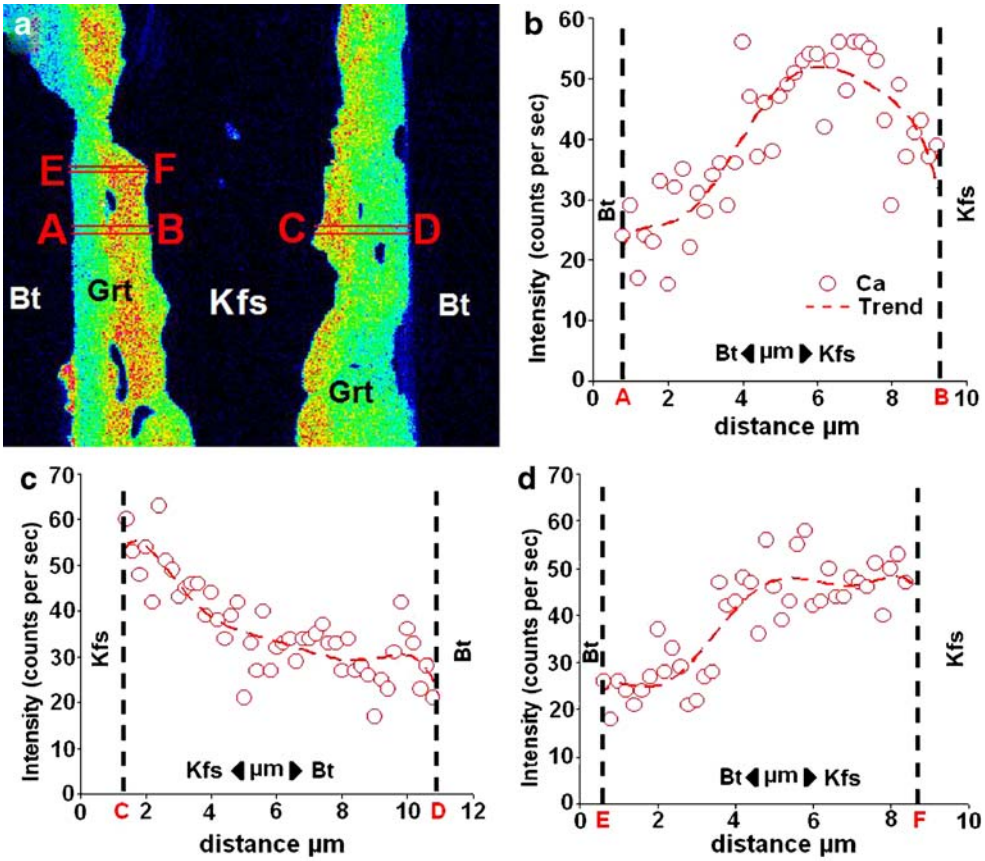

Fig. 5 The qualitative profiles for the Ca concentration across two garnet rims for sample D2_II. **a**) The element distribution map for Ca shows the locations of the qualitative profiles. **b**) Garnet composition along profile A-B. **c**) Garnet composition along profile C-D. **d**) Garnet composition along profile E-F. The vertical dashed lines indicate the perthite/garnet and the garnet/biotite interphase boundaries

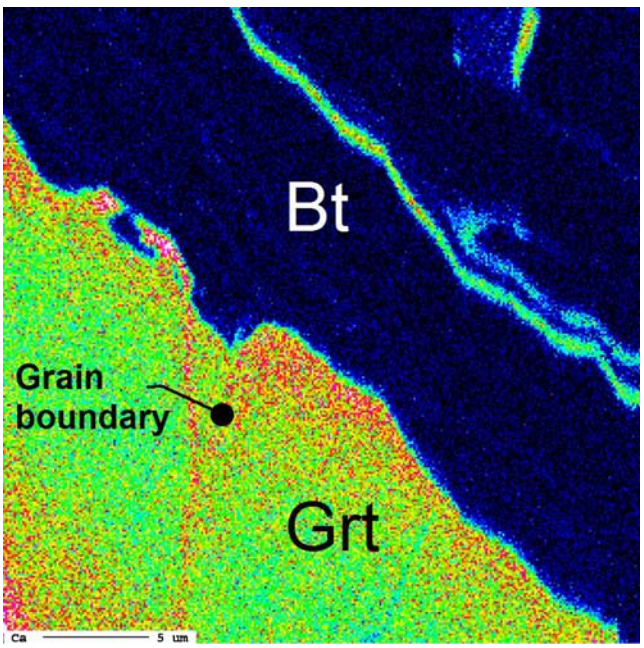

Fig. 6 FEMP map for Ca. Warm colours show a high concentration of Ca. The chemical transport along an assumed grain boundary is shown

We used the following parameter values. The ratio between grain boundary and volume diffusion in the garnet rim was set to $D_{Ca}^{gb}/D_{Ca}^{vol}=2 \bullet 10^3$; the diffusivity of Ca in plagioclase is considered to be faster by three orders of magnitude than within garnet so that $D_{Ca}^{Pl}/D_{Ca}^{Gt}=10^3$. Plagioclase is treated as reservoir for Ca with finite size. The ratio r/a between the size r of the model domain in the growth direction of the reaction rim and the boundary width a was set to the constant value of 10^4. Lastly, we assumed a similar component solubility in garnet and in the grain boundary medium. The only adjustable parameter was the spacing Ly between the grain boundaries in the y-direction (Fig. 8a).

In Figure 8 we show the Ca-zoning patterns that were obtained from finite difference modelling of garnet rim growth taking into account simultaneous grain boundary and volume diffusion. The calculated concentration profiles in Fig. 8b reflect different spacing of the grain boundaries in the y-direction, normalized to the size r of the model domain in the growth-direction.

Discussion

The growth of continuous reaction rims between reactants, in general, requires material transfer across the growing

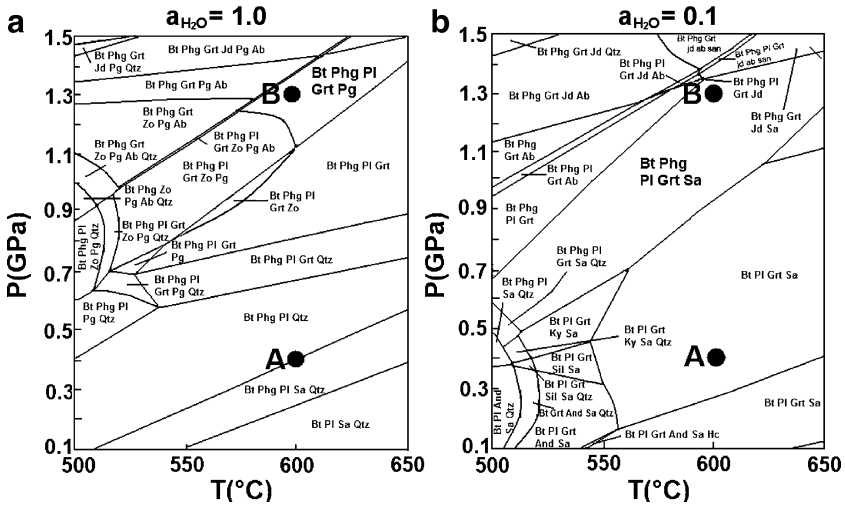

Fig. 7 Equilibrium phase relations calculated for a bulk rock composition consisting of equal amounts of 1/2 plagioclase and 1/2 biotite for sample 284-1. Phase diagram calculations for aH_2O=1.0 (**a**) and aH_2O= 0.1 (**b**) were done using the Vertex program of Connolly (1990) Thermodynamic data were taken from Holland and Powell (1998). The diagrams show albite (Ab), andalusite (And), biotite (Bt), garnet (Grt), hercynite (Hc), jadeite (Jd), paragonite (Pg), phengite (Phg), plagioglase (Pl), quartz (Qtz), sanidine (Sa) and zoisite (Zo). (A) Point of Permian metamorphism at 600 °C and 0.4 GPa. (B) Point of Eo-Alpine eclogite facies metamorphic overprint at 600 °C and 1.3 GPa

rim, which is considered to occur by volume diffusion (Thompson 1959, Joesten 1977). In the present example, the growth of the garnet rims requires transfer of FeO and MgO components from the garnet-biotite interfaces to the garnet-plagioclase or the garnet-perthite interface and the transport of the CaO component in the opposite direction. If rim growth is controlled by such bi-directional transport of FeO + MgO and CaO, garnet growth is expected to occur from the original biotite-feldspar contact in both directions (Joesten 1977, Abart et al. 2001). In the example described here, garnet growth likely occurred at similar rates at both reaction interfaces as is indicated by the location of a pronounced chemical gradient in the inner garnet rims. The location of such a chemical gradient roughly coincides with the location of the original plagioclase-biotite phase boundary (Keller et al. 2006, 2008) came to the same conclusions based on microstructural evidence observed in similar garnet reaction rims from the Monte Rosa area (Western Alps). There complex Ca zoning across garnet reaction rims was explained with characteristics similar to those found in the samples from the Saualpe. A slight increase in Ca concentrations at the garnet-biotite interface is ascribed to fast transport of the CaO component from the garnet-feldspar interface towards the garnet-biotite interface along garnet grain boundaries (Keller et al. 2006). Keller et al. (2006) and Keller et al. (2008) demonstrated by numerical modelling that this type of Ca zoning can only be produced if the diffusivity of Ca within the transport

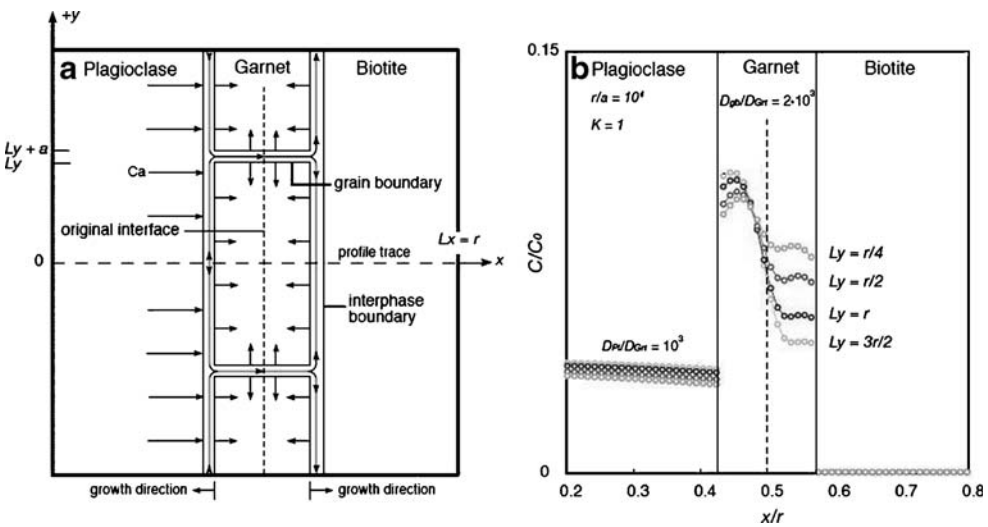

Fig. 8 Schematic drawing of the garnet rim growth model containing parallel grain boundaries (**a**) and calculated concentration profiles (**b**); (**a**) The arrows mark the direction of Ca-flux, variable arrow lengths indicate differing transport rates along various chemical pathways; (**b**) calculated Ca-concentration profiles (profile trace: y=0) show the dependence of the evolving concentration profile on the spacing between the grain boundaries (i.e. value of *Ly*)

medium along the 1–2 nm wide grain boundaries is faster than the diffusivity of Ca through the grain interiors by a factor of 10^3 to 10^5. If mass transport along grain boundaries were less efficient, this would produce Ca zoning with monotonously decreasing Ca concentrations from the garnet-feldspar to the garnet-biotite interface. If mass transfer along grain boundaries were more efficient than that, the produced garnet reaction rims would be essentially chemically homogeneous. Calcium zoning across the garnet rim is thus a sensitive monitor for the relative contributions of both grain boundary diffusion and volume diffusion to bulk material transfer across the growing rim.

In the samples from the Saualpe complex both types of Ca zoning were observed within one sample. These include monotonous decrease of Ca concentrations from the garnet-feldspar to the garnet-biotite interface, as well as more complex Ca zoning with the highest Ca concentrations approximately along the central axis of the rim, decreasing Ca concentrations towards the feldspar, and slightly elevated Ca concentrations at the garnet-biotite interface. These differences in Ca zoning patterns reflect local variations in the relative contribution of grain boundary diffusion to bulk material transfer across the growing garnet rim. The contribution of grain boundary diffusion to bulk mass transfer depends on the transport efficiency of the component in the grain-boundary medium, as reflected by the grain boundary diffusion coefficient D^{gb}, and the solubility of the component within the grain boundary medium. It further depends on the cross sectional area that is occupied by the grain boundary medium as compared to the cross sectional area that is occupied by the mineral grains. The fraction of cross sectional area occupied by the grain boundary medium depends on grain boundary width and on the spacing between grain boundaries. Because local variations in transport efficiency along grain boundaries, due to variations in grain boundary diffusivities and solubility or due to local variations in grain boundary width are unlikely, we propose that differences in the spacing between grain boundaries were responsible for the different Ca zoning patterns. Figure 8b shows that for a large spacing between the grain boundaries the Ca zoning is characterized by a close to monotonous decrease in the Ca concentration from the garnet-plagioclase to the garnet-biotite interface. The zoning becomes more complex and a slight increase in the Ca concentration develops from the central axis of the rim towards the garnet-biotite interface, if the spacing between the grain boundaries is decreased. When reducing the spacing between grain boundaries, the efficiency of material transfer across the reaction rim, and thus the availability of Ca at the garnet-biotite reaction interface, is increased. This allows for the formation of a Ca enriched garnet at this interface and explains the difference between the Ca concentrations in the relatively Ca rich and Ca poor domains of the garnet rim and the difference in Ca depletion in the adjacent plagioclase. For each of the assumed spacings between the grain boundaries, the modelled Ca concentration is highest approximately in the middle between the centre of the garnet rim and the garnet-plagioclase interface. The highest Ca concentration moves slightly towards the centre of the garnet rim with decreasing spacing between the grain boundaries. In addition, the Ca concentration shows a systematic decrease towards the garnet-plagioclase interface. This is due to the fact that the Ca source gets successively more exhausted during garnet rim growth such that later garnet growth stages occur under conditions of continuing Ca depletion. This effect is also visible at the garnet-biotite interface, albeit less pronounced. The formation of Ca depletion halos in plagioclase, during the growth of similar garnet reaction rims, has also been documented by Keller et al. (2006).

Conclusions

From complex chemical zoning patterns in garnet reaction rims that formed in biotite-plagioclase gneisses along pre-existing biotite-plagioclase or biotite-perthite contacts, we infer that mass transfer across the growing rims occurred by a combination of volume diffusion through the grain interiors coupled with grain boundary diffusion. Short circuit diffusion along grain boundaries may produce complex chemical zoning with non-monotonous concentration variations across the garnet rim. Such complex zoning is particularly pronounced for Ca in the garnet rims from the Saualpe complex. The contribution of grain boundary diffusion relative to bulk mass transfer across the growing rims depends, among others, on the fraction of the cross sectional area that is occupied by the grain boundaries. It is argued, that local variations in the Ca zoning patterns seen in the garnet rims are due to differences in the spacing between grain boundaries.

Acknowledgments Access to the facilities of the electron microprobe laboratory at Free University of Berlin and the electron microprobe laboratory at GFZ Potsdam is gratefully acknowledged. Thanks to R. Milke and D. Rhede for that possibility and their help at the microprobe. The reviewers G. Hoinkes and G. Habler are thanked for their extensive critical and constructive comments, which were very helpful to improve the paper. D. Harlov is thanked for his editorial handling of the paper and his helpful comments. At last J. Raith is thanked for a final review of the paper. Funding of this work with the DFG research project AB 314/2-1 in the framework of the DFG research group FOR 741 is gratefully acknowledged.

References

Abart R, Martinelli W (1989) Alpidische und variszische Entwicklungsgeschichte des Wölzer Kristallins. Mitt Ges Geol Bergbaustud Österr 37:1–14

Abart R, Schmid R, Harlov D (2001) Metasomatic coronas around hornblendite xenoliths in granulite facies marbles, Ivrea Zone, N-Italy I: constraints on component mobility. Contrib Mineral Petrol 141:473–493

Connolly JAD (1990) Multivariable phase diagrams: an. algorithm based on generalized thermodynamics. Am J Sci 290:666–718

Fisher GW (1973) Nonequilibrium thermodynamics as a model for diffusion controlled metamorphic processes. Am J Sci 273:897–924

Frank W, Elsterlus M, Jung G, Krohe A, Weber J (1983) Die Entwicklungsgeschichte von Stub- und Koralpenkristallin und die Beziehung zum Grazer Paläozoikum. Jahresbericht 1982 Hochschulschwerpunkt 15:263–293

Gaidies F, Abart R, de Capitani C, Schuster R, Connolly JAD, Reusser E (2006) Characterisation of polymetamorphism in the Austroalpine basement east of the Tauern Window using garnet isopleth thermobarometry. J Metamorph Geol 24:451–475

Gaidies F, de Capitani C, Abart R, Schuster R (2007) Prograde garnet growth along complex P-T-t paths: results from numerical experiments on polyphase garnet from the Wölz Complex (Austrolalpine basement). Contrib Mineral Petrol 155:673–688

Habler G (1999) Die polyphase Metamorphose- und Strukturprägung der Eklogitführenden Kristallineinheiten im Raum Knappenberg (NW Saualpe, Kärnten). Unpublished M.Sc.Thesis, University of Viena

Habler G, Thöni M (2001) Preservation of Permo-Triassic low-pressure assemblages in the Cretaceous high-pressure metamorphic Saualpe crystalline basement (Eastern Alps, Austria). J Metamorph Geol 19:679–697

Habler G, Thöni M, Miller C (2007) Major and trace element chemistry and Sm-Nd age correlation of magmatic pegmatite garnet overprinted by eclogite-facies metamorphism. CG 241:4–22

Heede H-U (1997) Isotopengeologische Untersuchungen an Gesteinen des ostalpinen Saualpenkristallins, Kärnten-Österreich. Münster Forsch Geol Paläont 81:1–168

Holland TJB, Powell R (1998) An internally consistent thermodynamic data set for phases of petrological interest. J Metamorph Geol 16:309–343

Joesten R (1977) Evolution of mineral assemblage zoning in diffusion metasomatism. Geochim Cosmochim Acta 41:649–670

Keller L, Abart R, Wirth R, Schmid D, Kunze K (2006) Enhanced mass transfer through short circuit diffusion: growth of garnet reaction rims at eclogite facies conditions. Am Mineral 91:1024–1038

Keller L, Wirth R, Rhede D, Kunze K, Abart R (2008) Asymmetrically zoned reaction rims: the key to assess grain boundary diffusivities and growth rates related to natural diffusion controlled mineral reactions. J Metamorph Geol 26:99–120

Lichem et al (1997) Polymetamorphism of the Austroalpine Koralm Basement: New Evidence for a Permian Event. Terra Abstracts 9/1: EUG IX 489

Miller C, Thöni M (1997) Eo-alpine eclogitisation of permian MORB-type gabbros in the Koralpe (Eastern Alps, Austria): new geochronological, geochemical and petrological data. Chem Geol (Isotope Geoscience Section) 137:283–310

Morauf W (1980) Die permische Differentiation und die alpidische Metamorphose des Granitgneises von Wolfsberg (Koralpe) mit Rb-Sr- und K-Ar-Isotopenbestimmung. Tschermaks Miner Petrogr Mitt 27:169–185

Morauf W (1981) Rb-Sr- und K-Ar-Isotopen-Alter an Pegmatiten aus Kor- und Saualpe, SE-Ostalpen. Österreich. Tschermaks Miner Petrogr Mitt 28:113–129

Morauf W (1982) Rb-Sr- und K-Ar-Evidenz für eine intensive alpidische Beeinflussung der Paragesteine in Kor- und Saualpe, SE-Ostalpen, Österreich. Tschermaks Miner Petrogr Mitt 29:255–282

Paquette J-L & Gebauer D (1991) U-Pb zircon and Sm-Nd isotopic study on eclogitized meta-basic and meta-acidic rocks of the Koralpe, Eastern Alps, Austria. Terra Abstracts 3/1:EUG VI 505

Pilger A, Schönenberg R (1975) Geologie der Saualpe. Claust Geol Abh Sonderband 1

Schmid SM, Fügenschuh B, Kissling E, Schuster R (2004) Tectonic map and overall architecture of the Alpine orogen. Eclogae Geologicae Helvetiae 97:61–77

Schuster R, Thöni M (1996) Permian garnets: indication for a regional Permian metamorphism in the southern part of the Austroalpine basement units. Mitt Ges Geol Bergbaustud Österr 141:219–221

Schuster R, Schabert S, Abart R, Frank W (2001) Permo-Triassic extension and related HT/LP metamorphism in the Austroalpine-Southalpine realm. Mitt Ges Geol Bergbaustud Österr 45:111–141

Schuster R, Stüwe K (2008) Permian metamorphic event in the Alps. Geology 36:603–608

Thompson JB Jr (1959) Local equilibrium in metasomatic processes. Res Geochim 1:427–457

Thöni M, Jagoutz E (1992) Some new aspects of dating eclogites in orogentic belts:Sm-Nd, Rb-Sr, and Pb-Pb isotopic results from the Austroalpine Saualpe and Koralpe type-locality (Carinthia/Styria, southeastern Austria). GCA 56:347–368

Thöni M, Jagoutz E (1993) Isotopic constraints for eo-Alpine high-P metamorphism in the Austroalpine nappes of the Eastern Alps, bearing on Alpine orogenesis. Schweiz Mineral Petrogr Mitt 73:177–189

Thöni M, Miller C (2000) Permo-Triassic pegmatites in the eo-Alpine eclogite-facies Koralpe complex, Austria: age and magma source constraints from mineral chemical, Rb-Sr and Sm-Nd isotope data. Schweiz Mineral Petrogr Mitt 80:169–186

Thöni M, Miller C (2008) Multi-stage garnet from the Plankogel unit, Eastern Alps: new constraints from Sm-Nd-Isotope, trace element and P-T-data. G R A 10:EGU2008–A–07141 EGU 2008